Cleavage of Cdc6 by caspase-3 promotes ATM/ATR kinase–mediated apoptosis of HeLa cells

Hyungshin Yim,[1] In Sun Hwang,[1] Joon-Seok Choi,[1] Kwang-Hoon Chun,[1] Ying Hua Jin,[2] Young-Mi Ham,[1] Kwang Youl Lee,[3] and Seung Ki Lee[1]

[1]Division of Pharmaceutical Biosciences, Research Institute for Pharmaceutical Sciences, College of Pharmacy, Seoul National University, Seoul 151-742, Korea
[2]College of Life Science, Jilin University, Changchun 130012, China
[3]College of Pharmacy, Chonnam National University, Gwangju 500-757, Korea

We show that caspase-3 cleaves Cdc6 at D^{290}/S and D^{442}/G sites, producing p32-tCdc6 (truncated Cdc6) and p49-tCdc6, respectively, during etoposide- or tumor necrosis factor (TNF)-α–induced apoptosis. The expression of these tCdc6 proteins, p32- and p49-tCdc6, promotes etoposide-induced apoptosis. The expression of tCdc6 perturbs the loading of Mcm2 but not Orc2 onto chromatin and activates ataxia telangiectasia mutated (ATM) and ATM and Rad-3 related (ATR) kinase activities with kinetics similar to that of the phosphorylation of Chk1/2. The activation kinetics are consistent with elevated cellular levels of p53 and mitochondrial levels of Bax. The tCdc6-induced effects are all suppressed to control levels by expressing a Cdc6 mutant that cannot be cleaved by caspase-3 (Cdc6-UM). Cdc6-UM expression attenuates the TNF-α–induced activation of ATM and caspase-3 activities. When ATM or ATR is down-expressed by using the small interfering RNA technique, the TNF-α– or tCdc6-induced activation of caspase-3 activities is suppressed in the cells. These results suggest that tCdc6 proteins act as dominant-negative inhibitors of replication initiation and that they disrupt chromatin structure and/or induce DNA damage, leading to the activation of ATM/ATR kinase activation and p53–Bax-mediated apoptosis.

Introduction

DNA replication is a key process that is functionally perturbed during DNA damage–triggered apoptosis (Burhans et al., 2003). DNA damage triggers apoptosis in a replication-dependent way by activating the mitochondrial damage pathway in fibroblasts (Kaina, 2003). Chromosomal replication can be impaired by intrinsic replication errors or by external agents that cause DNA damage (Hammond et al., 2002; Dodson et al., 2004).

Checkpoint-sensing kinases detect abnormal replication structures and activate the Chk2 kinase, which stabilizes replication forks and promotes recovery from DNA damage by phosphorylating downstream endonucleases, helicases, and recombinases, demonstrating that DNA replication forks are activators and effectors of the checkpoint pathway in S phase (Kai and Wang, 2003; Tercero et al., 2003). In response to a variety of DNA lesions in eukaryotic cells, DNA damage–sensing kinases such as ataxia telangiectasia mutated (ATM), ATM and

Rad-3 related (ATR), and DNA-dependent protein kinase are activated as checkpoint sensors that signal both the cell cycle and apoptosis machinery through the Chk1/2 checkpoint kinases (Liu et al., 2000; Matsuoka et al., 2000; Shiloh, 2003). ATM and Chk2 directly phosphorylate p53, a key regulator of cellular responses to genotoxic stress. Phospho-p53 can then dissociate with the inhibitor protein Mdm2 and, thus, is stabilized and transcriptionally activated for DNA damage responses (Shiloh, 2003; Pereg et al., 2005). The p53 protein also has a transcription-independent activity that potentiates cell death once transcription-dependent functions initiate this process (Haupt et al., 2003). Cytoplasmic p53 directly activates the proapoptotic protein Bax through direct interaction (Schuler et al., 2000; Chipuk et al., 2004).

Several lines of evidence indicate that replication initiation is impaired in the early stages of apoptosis. First, apoptosis is induced by defects in the initiation of DNA replication as a result of the o*rc2-1* mutation (Weinberger et al., 2005). In addition, temperature-sensitive *orc2-1* mutants cause a defect in a checkpoint and initiation of DNA replication (Weinberger et al., 1999; Trabold et al., 2005). Second, replication initiation

proteins such as Cdc6 and Mcm3 are cleaved by caspase early in apoptosis (Blanchard et al., 2002; Pelizon et al., 2002; Yim et al., 2003; Schories et al., 2004). Third, when the expression of proteins such as Cdc6, Mcm2, and Cdc45 is blocked by the siRNA technique, proliferation is inhibited, and apoptosis is induced in cancer cells (Feng et al., 2003). Thus, replication fork collapse induced by interfering with the pre–replicative complex (RC) may be a general feature of the early stages of apoptosis.

In a previous study, we showed that caspase-3–mediated cleavage of Cdc6 induces the nuclear retention of the truncated protein p49-tCdc6 (truncated Cdc6) and apoptosis (Yim et al., 2003). We proposed that p49-tCdc6 acts as a dominant-negative inhibitor of replication that consequently induces and enhances apoptosis. In this study, we show that Cdc6 is also specifically cleaved during apoptosis by caspase-3 at another aspartic acid residue, D290, yielding a truncation protein (p32-tCdc6) that accumulates in the nucleus under conditions in which cyclin A/Cdk2 activity is up-regulated. Interestingly, the expression of p32-tCdc6 or p49-tCdc6 markedly increases apoptosis in etoposide-treated cells and induces apoptosis of untreated cells. Moreover, the expression of tCdc6 proteins induces activation of the ATM and ATR kinase. The expression of tCdc6 also suppresses the

chromatin loading of the replication initiation factor Mcm2. Importantly, tCdc6-induced effects are prevented in cells that coexpress a version of Cdc6 that cannot be cleaved by caspase-3 (Cdc6-UM). Moreover, when ATM or ATR is down-expressed using the siRNA technique, caspase-3 activity is suppressed in TNF-α–induced cells. These results suggest that the caspase-mediated cleavage of Cdc6 destabilizes the pre-RC and, thus, that tCdc6 proteins impair replication initiation by acting as dominant-negative inhibitors. This, in turn, results in the disruption of chromatin structure and/or induction of DNA damage, leading to ATM/ATR kinase–mediated apoptosis.

Results

Cdc6 is specifically cleaved at two sites by caspase-3 during etoposide-induced apoptosis

In etoposide-induced apoptosis of HeLa cells, the 62-kD Cdc6 protein is specifically cleaved into fragments of 49 and ∼36 kD, with kinetics similar to that of the proteolytic cleavage of poly (ADP-ribose) polymerase (PARP; Fig. 1 A). Cleavage at SEVD[442]/G produces p49-tCdc6. To identify the second Cdc6
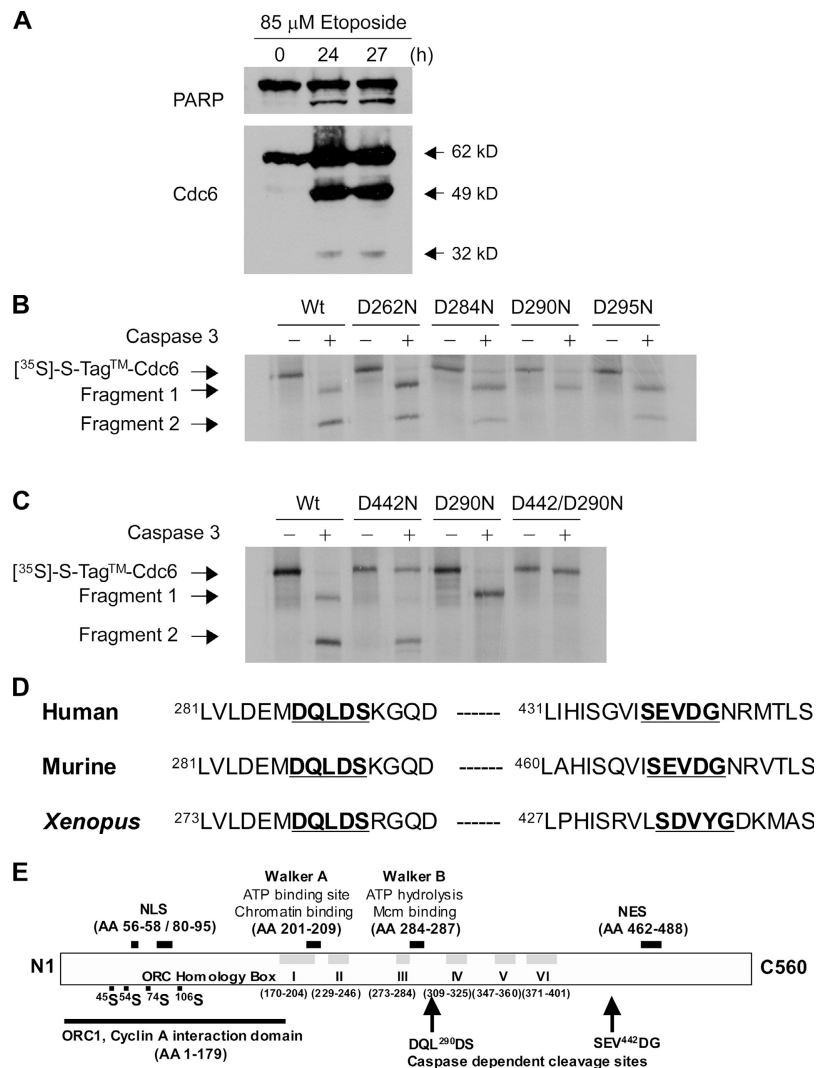

Figure 1. **Caspase-3 specifically cleaves Cdc6 at two sites during etoposide-induced apoptosis.** (A) Cdc6 undergoes specific cleavages in HeLa cells treated with 85 μM etoposide. Nuclear extracts were resolved by 12% SDS-PAGE and subjected to immunoblot analysis using anti-Cdc6 and anti-PARP antibodies. (B and C) Mutant and wt Cdc6 proteins were translated in vitro in the presence of [35S]methionine and incubated at 30°C for 1 h with recombinant caspase-3. The reaction mixtures were resolved by 12% SDS-PAGE and visualized by autoradiography. (D) Comparison of Cdc6 amino acid sequences and caspase-3 cleavage sites (underlining) from different species. (E) Caspase-3 cleavage sites and functional domains of human Cdc6 that are responsible for interactions with other proteins are indicated.

cleavage site, we constructed mutants in which asparagine is substituted for aspartic acid at one candidate site (DQLD^{290}/S) and at three other sequences (AGKD^{262}/M, LVLD^{284}/E, and KGQD^{295}/V) that are all in a region where cleavage would produce a fragment of ~36 kD. Recombinant caspase-3 efficiently cleaved wild-type (wt) Cdc6 (Cdc6-wt) and the D262N, D284N, and D295N mutant proteins into 49- and 32-kD fragments (Fig. 1 B). In contrast, the D290N mutant was not cleaved, and this cleavage site was further confirmed with the double mutant protein D442N/D290N, which was resistant to caspase-3 cleavage, indicating that aspartic acid residues 290 and 442 are caspase-3 cleavage sites during apoptosis (Fig. 1 C).

Interestingly, a 15–amino acid residue region including the DQLD^{290}/S cleavage site is well conserved among man, mouse, and *Xenopus*, whereas the region including the SEVD^{442}/G site is more loosely conserved (Fig. 1 D). Moreover, p32-tCdc6 and p49-tCdc6 contain all functional domains that are known to be essential for pre-RC loading (Fig. 1 E).

The cytoplasmic export of tCdc6 proteins is suppressed

We then assessed whether the p32-tCdc6 protein is functional for translocation into the cytoplasm because caspase cleavage removes the COOH-terminal nuclear export signal (NES) sequences. pCS2+GFP-tagged Cdc6-wt, tCdc6, or Cdc6-AAA, which is an unphosphorylatable mutant of Cdc6 on 54, 74, and 106 serines, was cotransfected with pCMV-mock, cyclin A, or dominant-negative Cdk2 into HeLa cells. Cdc6-wt was translocated to the cytoplasm when cyclin A was coexpressed, whereas Cdc6-AAA was not even if cyclin A was coexpressed (Fig. 2, A and B). Although the cytoplasmic translocation of

Cdc6-wt was mainly regulated by cyclin A/Cdk2-mediated phosphorylation (Fig. 2, A and B), the cytoplasmic translocation of p32-tCdc6 was relatively independent of cyclin A/Cdk2 activity. The p32-tCdc6 protein was localized in the nucleus in 92% of the cells cotransfected with pCMV-mock, a higher percentage than for cells expressing p49-tCdc6 or Cdc6-wt (87 and 68%, respectively).

The differential distribution of p32-tCdc6 and p49-tCdc6 was more significant when cyclin A was coexpressed. Under conditions of elevated cyclin A/Cdk2 activity, the cytoplasmic trans-localization of p32-tCdc6 was suppressed by 78% as compared with that of Cdc6-wt (94 − 16%, because 94% of Cdc6-wt and 16% of p32-tCdc6 was localized in the cytoplasm). Under the same conditions, the translocation of p49-tCdc6 was suppressed by 57% (94 − 37%), as 37% of p49-tCdc6 was localized in the cytoplasm. Thus, p32-tCdc6 was more strongly retained in the nucleus (by 21%; 78 − 57%) as compared with the p49-tCdc6 protein under conditions of up-regulated cyclin A/Cdk2 activity. These results indicated that the p49-tCdc6 protein might contain an additional NES-like sequence between amino acid residues 290 and 442. In contrast, the cytoplasmic export of p49-tCdc6 and p32-tCdc6 was almost completely prevented, as was the translocation of Cdc6-wt in cells expressing Cdk2-DN, resulting in nuclear localization in 99% of the transfected cells (Fig. 2, A and B).

Together, our data indicate that the phosphorylation of Cdc6-wt and tCdc6 proteins is essential for their cytoplasmic translocation and that the loss of a NES-like sequence from p49-tCdc6 reduces phosphorylation-dependent translocation. Our results showed that the majority of Cdc6-wt was translocated to the cytoplasm, whereas the Cdc6-AAA mutant protein
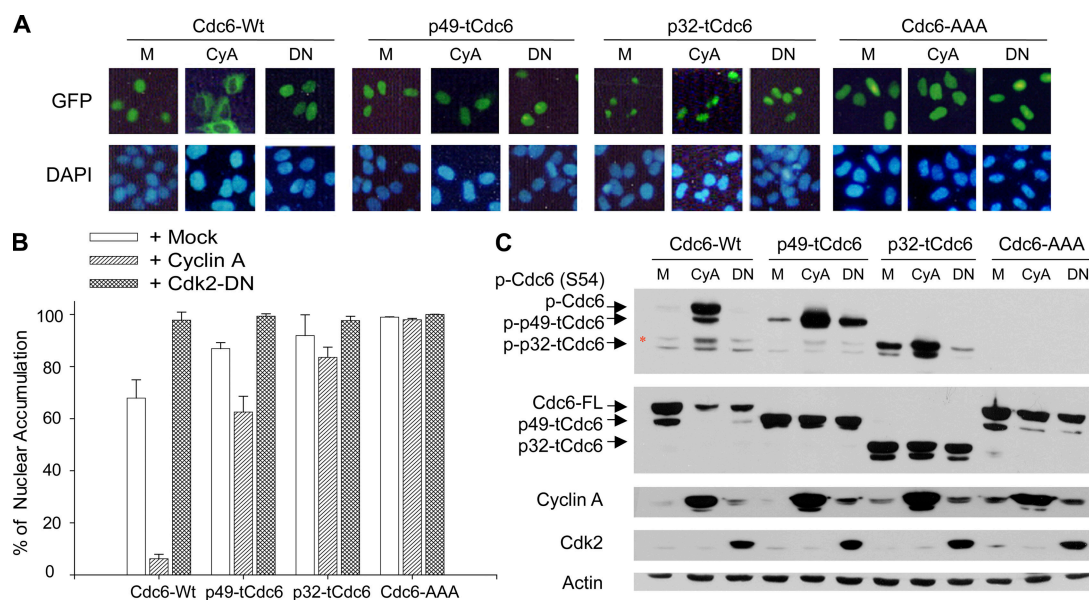

Figure 2. **Cleavage of Cdc6 induces nuclear accumulation of tCdc6 proteins.** Cells were cotransfected with 1.5 μg each of pCS2+GFP–Cdc6-wt, –p49-tCdc6, –p32-tCdc6, or –Cdc6-AAA and 1.5 μg each of pCMV-mock (M), pCMV–cyclin A (CyA), or dominant-negative pCMV-Cdk2 (DN) as indicated. (A) After 24 h, cells were fixed and stained with DAPI. (B) The percentages of transfected cells in which Cdc6-wt, tCdc6, or Cdc6-AAA protein localizes to the nucleus were determined; data are expressed as means ± SD (error bars) from three determinations obtained in each of three experiments. (C) After 24 h, cell extracts were prepared, resolved by 10% SDS-PAGE, and subjected to immunoblot analysis with specific antibodies against p-Cdc6 (S54), Cdc6, cyclin A, Cdk2, and actin. An asterisk denotes endogenous Cdc6.

was mainly retained in the nucleus even if cyclin A was co-expressed in the cells (Fig. 2, A and B). Also, Cdc6-wt, p49-tCdc6, and p32-tCdc6 but not Cdc6-AAA were all similarly phosphorylated when they were prepared from cells that coexpressed cyclin A. Phosphorylation was prevented in cells expressing Cdk2-DN (Fig. 2 C). Thus, tCdc6 proteins were similarly phosphorylated, but their phosphorylation-dependent cytoplasmic translocation was impaired by the loss of NES-like sequences in the region of 300–315 amino acid sequences.

Expression of tCdc6 proteins induces apoptosis and enhances the etoposide-induced apoptosis of HeLa cells

We next tested the effect of p32-tCdc6 or p49-tCdc6 expression on apoptosis. Indeed, the expression of p32-tCdc6 notably enhanced etoposide-induced cell death to a greater extent than that of p49-tCdc6 (Fig. 3, A–C). The expression of either protein markedly increased the number of cells with apoptotic morphology (membrane blebbing and cell shrinkage) to 95 and 79%, respectively, whereas such changes occurred in <32% of cells expressing Cdc6-wt (Fig. 3 A). Similarly, the numbers of cells expressing tCdc6 that exhibited condensed DNA or that were Annexin V$^+$ and propidium iodide$^-$ (PI$^-$) also significantly increased after treatment with etoposide (Fig. 3, B and C). In all cases, the apoptosis-promoting effects of p32-tCdc6 expression were higher than those induced by p49-tCdc6 expression. In addition, when pCS2+GFP-tagged p49- and

p32-tCdc6 (1.5 µg cDNA of each) were cotransfected, the apoptosis-promoting effect was slightly lower than that induced by p32-tCdc6 (3 µg cDNA) but significantly higher than that induced by the same amount of p49-tCdc6 cDNA (Fig. 3, A–C). Also, apoptosis was clearly induced in cells expressing p32-tCdc6 under normal HeLa cell culture conditions. The number of cells with apoptotic cell morphology increased by 78 and 63% from 24 to 48 h after transfection in p32-tCdc6– or p49-tCdc6–expressed cells, respectively, whereas the expression of Cdc6-wt had a minimal effect (Fig. 3 D). Moreover, the sub-G1 proportion of cells expressing GFP-tagged p32-tCdc6 increased to 21% over the course of 48 h, whereas <10% of cells expressing Cdc6-wt or the vector alone were in this sub-G1 proportion (Fig. 3 E). In addition, the Annexin V assay showed that the early apoptotic population of cells expressing p32-tCdc6 increased by three- to fourfold as compared with cells overexpressing Cdc6-wt or the vector 48 h after transfection (Fig. 3 F). When p49- and p32-tCdc6 were coexpressed in the cells, the apoptosis-inducing effect increased in a time-dependent manner over the 48 h (Fig. 3, D–F). The results indicated that in the coexpressed cells, the apoptosis-inducing effect is even higher than those induced by expressing p49- or p32-tCdc6 alone 48 h after transfection. Thus, the expression of tCdc6 proteins induces apoptosis in HeLa cells under normal cell culture conditions, and the differential effects of the two truncated versions of Cdc6 are consistent with their relative impairments in export from the nucleus.
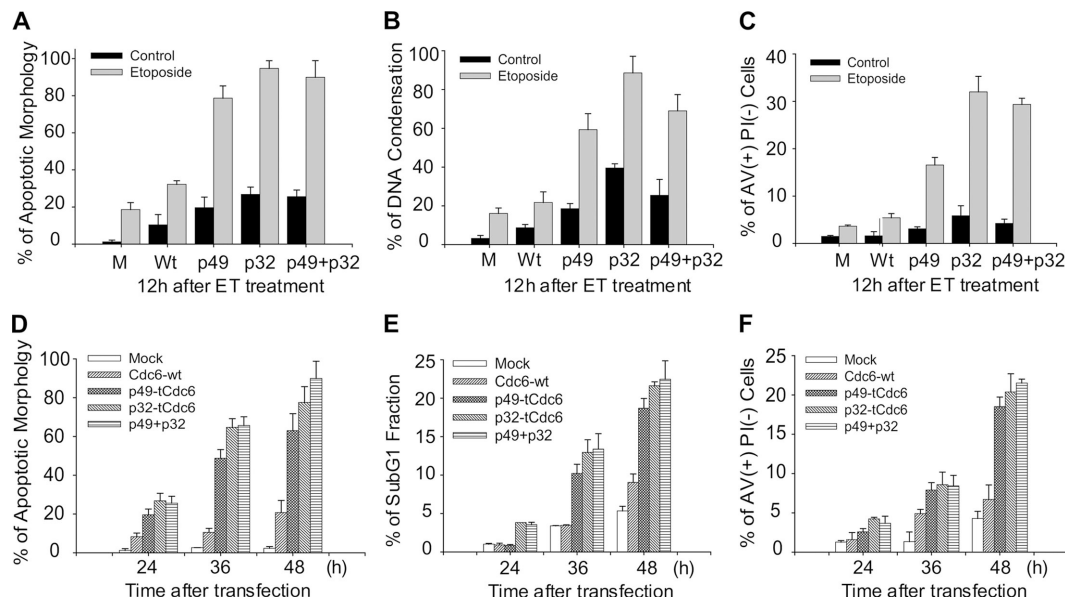

Figure 3. **Expression of tCdc6 proteins induces apoptosis and enhances etoposide-induced apoptosis in HeLa cells.** (A–C) HeLa cells were transfected with 3 µg pCS2+GFP-tagged Cdc6-wt or tCdc6 and incubated for 24 h, which were then treated with 85 µM etoposide (ET) for 12 h. For the cotransfection study, 1.5 µg of each pCS2+GFP–p49- and p32-tCdc6 was used. (A) The percentage of GFP-expressed cells showing membrane blebbing was determined after treatment with etoposide. (B) Transfected cells were stained with DAPI after treatment with etoposide, and the percentage of GFP-expressed cells with condensed DNA was quantified. (C) The Annexin V assay was performed with the transfectants after treatment with etoposide as described in Materials and methods. The percentage of early apoptotic cells was calculated and is represented as a histogram. (D–F) HeLa cells were transfected with 3 µg pCS2+GFP-Cdc6. When p49- and p32-tCdc6 were coexpressed, 1.5 µg cDNA of each was used. (D) The images of transfected cells were collected by fluorescence microscopy 24, 36, and 48 h afterward. The percentage of GFP-expressed cells showing membrane blebbing was quantitated. (E) FACS analysis was performed in a time-dependent manner after transfection. The proportion of cell populations in the sub-G1 among GFP$^+$ cells was calculated and is represented as a histogram. (F) The Annexin V assay was performed with transfectants expressing GFP in a time-dependent manner. The means ± SD (error bars) of data from at least three experiments are shown.

Caspase-mediated cleavage of Cdc6 interferes with pre-RC loading

To assess the functional relevance of the caspase-mediated cleavage of Cdc6, we first tested its effect on pre-RC loading. Both p49- and p32-tCdc6 bound chromatin with kinetics similar to that of PARP cleavage in cells treated with etoposide or TNF-α (Fig. 4, A and B). The kinetics of binding indicated that p49-tCdc6 bound before p32-tCdc6. Moreover, chromatin-bound Mcm2 levels were strongly reduced, whereas the levels of chromatin-bound Orc2 remained unaltered in cells treated with etoposide or TNF-α. In addition, the reduced levels of chromatin-bound Mcm2 temporally correlated with elevations in the level of chromatin-bound tCdc6 proteins (Fig. 4, A and B). Thus, the caspase-dependent cleavage of chromatin-bound Cdc6 interfered with the binding of Mcm2 binding onto chromatin, but cleavage did not prevent tCdc6 proteins from binding chromatin. Also, ectopically expressed tCdc6 proteins were specifically incorporated onto chromatin and subsequently inhibited the binding of Mcm2 to chromatin, but they did not interfere with the loading of Orc2 onto chromatin in both asynchronized and early S phase cells (Fig. 4 C). Our results also indicate that the interaction of Mcm2 with tCdc6 proteins was markedly reduced as compared with the Mcm2–Cdc6-wt interaction in transfected cell extracts (Fig. 4 D). The cellular levels of Cdc6-wt and tCdc6 proteins were largely equivalent. In summary, these results indicate that the binding of tCdc6 proteins to chromatin

interferes with the loading of DNA replication initiation factors, including Mcm2, onto replication complexes, thereby hindering the initiation of replication.

Expression of tCdc6 proteins induces apoptosis that involves DNA damage–sensing kinase activation and elevation of p53–Bax complex formation

We then determined whether the tCdc6-induced impairment of Mcm2 loading onto chromatin is functionally linked to ATM and ATR kinase activities (Fig. 5 A). Interestingly, in cells expressing tCdc6, ATR and ATM kinase activities significantly increased in a time-dependent fashion 24–36 h after transfection, whereas their cellular protein levels were minimally altered. Moreover, in cells expressing tCdc6, the phosphorylated levels of Chk1 on S345 residue and Chk2 on T68 also markedly increased, with kinetics similar to those of the increases in ATM and ATR kinase activities (Fig. 5 B). In addition, the extent of phosphorylation on the S15 residue of p53, which is phosphorylated by ATM kinase, increased in parallel with increases in the p53 protein level in cells expressing tCdc6. These results indicate that the expression of tCdc6 is likely to disturb chromatin structures and/or induce DNA damage, leading to ATM and ATR kinase activation and, thus, to p53 protein stabilization during apoptosis.

The protein levels of Bax and p21, which are target molecules of p53, also increased under the same conditions,
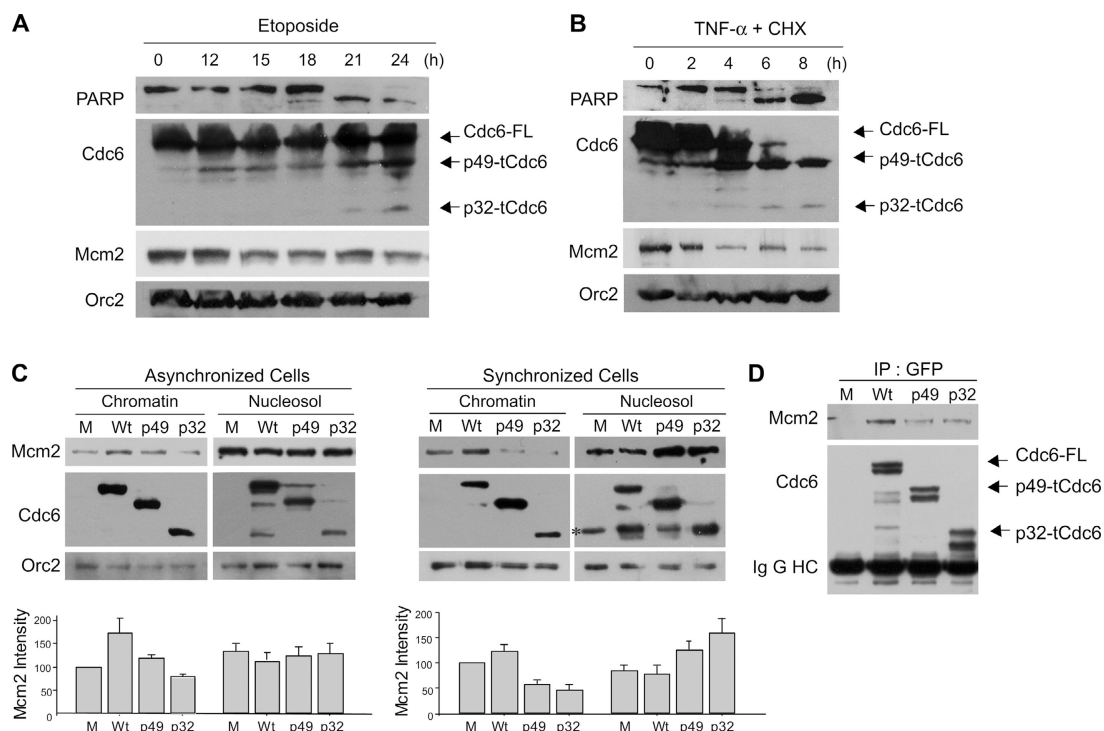

Figure 4. **Truncation of the chromatin-bound Cdc6 inhibits loading of Mcm2 onto chromatin during etoposide- or TNF-α–induced apoptosis.** (A and B) HeLa cells treated with etoposide or TNF-α and cycloheximide (CHX) were collected, and nuclear fractions were isolated. Chromatin fractions were separated as described in Materials and methods, and chromatin-bound proteins were detected with specific antibodies against Cdc6, PARP, Mcm2, and Orc2. (C) HeLa cells were transfected with 3 μg pCS2+GFP-tagged Cdc6-wt or tCdc6. After incubating for 24 h, asynchronized transfected cells or transfected cells that were synchronized in early S phase by treatment with hydroxyurea for 24 h were harvested. Chromatin and nucleosol proteins were resolved by SDS-PAGE and subjected to immunoblot analysis using specific antibodies against Cdc6, Orc2, and Mcm2. Error bars represent SD. (D) HeLa cell extracts were prepared 24 h after transfection and immunoprecipitated with an anti-GFP monoclonal antibody. Immunoprecipitates were resolved by SDS-PAGE and subjected to immunoblot analysis using the anti-Mcm2 and anti-Cdc6 antibodies. An asterisk denotes endogenous Cdc6.

indicating that the increased p53 level was functionally linked to induce Bax and p21 expression in tCdc6-expressing HeLa cells (Fig. 5 C). We next assessed the mitochondrial levels of Bax in cells expressing Cdc6-wt or tCdct6, as Bax is known to translocate to mitochondria during apoptosis (Gross et al., 1998). As shown in Fig. 5 C, the mitochondrial levels of Bax in cells expressing tCdc6 increased in a time-dependent manner, whereas the levels of mitochondrial VDAC, a mitochondrial marker protein, were unaltered. These results indicate that the mitochondrial translocation of Bax is promoted in cells expressing tCdc6 proteins. Interestingly, the levels of the p53–Bax complex were also notably elevated in cells expressing tCdc6, whereas the complex was almost undetectable in cells expressing the vector or Cdc6-wt (Fig. 5 D). Moreover, Bax in association with the p53 protein was detected as a double band in cells expressing tCdc6, whereas Bax that was unassociated with p53 was detected as a single band, suggesting that the upper band is a phosphorylated form (Fig. 5 D). These results also showed that the levels of mitochondrial Bax significantly increased in parallel with increases in the levels of p53 in transfected cells (Fig. 5 C). Interestingly, the levels of p53 in mitochondria also increased in concert with increases in mitochondrial Bax 36 h after transfection in tCdc6-expressed cells (Fig. 5 E). These results indicate that tCdc6 expression induces an elevation in the cellular levels of the p53–Bax complex and that this increase may be involved in the mitochondrial translocation of these proteins.

Proapoptotic effects induced by tCdc6 are effectively blocked in cells expressing the uncleavable mutant of Cdc6

We asked whether an uncleavable mutant of Cdc6 (Cdc6-UM) has the effects described for tCdc6 that disturb Mcm2 loading to the chromatin and activate DNA damage–sensing kinase activity and proapoptotic effect. As expected, Cdc6-UM was uncleaved, whereas Cdc6-wt was cleaved to p49-tCdc6 during TNF-α–induced apoptosis (Fig. 6 A). In addition, loading of the Mcm2 protein onto chromatin and ATR kinase activity were minimally influenced in cells expressing Cdc6-UM. In contrast, Mcm2 chromatin loading was suppressed, whereas ATR kinase activity was prominently up-regulated in cells expressing p49-tCdc6 or p32-tCdc6 (Fig. 6, B and C; top). However, the tCdc6-induced up-regulation of ATR kinase activity was markedly suppressed by coexpressing Cdc6-UM (Fig. 6 C, bottom). Moreover, the percentage of p32-tCdc6–expressing cells with apoptotic cell morphology decreased by ∼45% (79.7 − 34.5% = 45.2%) over the time course of 36–48 h after coexpression with Cdc6-UM (Fig. 6 D). These competition effects of Cdc6-UM on the tCdc6-induced events were similarly observed when the cells were coexpressed with Cdc6-wt and tCdc6 (Fig. 6, C and D). These results indicate that the expression of tCdc6 impairs Mcm2 loading onto chromatin, which is functionally linked to ATM/ATR kinase activation leading to apoptosis, and that these effects are blocked by the expression of Cdc6-UM.

Figure 5. **Expression of tCdc6 triggers DNA damage–induced apoptosis.** (A) HeLa cell extracts were prepared at various times after transfection, and ATM or ATR kinase was immunoprecipitated with anti-ATM or anti-ATR antibody, respectively. ATM or ATR kinase was assayed in vitro with PHAS-1 as a substrate in the presence of γ-[^{32}P]ATP, resolved by 15% SDS-PAGE, and followed by autoradiography. Proteins were also resolved by 8% SDS-PAGE and subjected to immunoblot analysis with specific antibodies against ATM, ATR, Cdc6, and actin. (B) HeLa cell extracts were prepared 30 h after transfection, and whole cell extracts were resolved by 10% SDS-PAGE and subjected to immunoblot analysis with specific antibodies against p53, p-p53 (S15), Chk1, pChk1 (S345), Chk2, pChk2 (T68), and actin. (C) Whole cell extracts and mitochondrial proteins were prepared at various times after transfection, resolved by 12% SDS-PAGE, and subjected to immunoblot analysis using specific antibodies against p53, Bax, p21, actin, and VDAC. (D) Whole cell extracts were prepared 30 h after transfection and immunoprecipitated with an anti-p53 polyclonal antibody, and immunoprecipitates were resolved by SDS-PAGE and subjected to immunoblot analysis using anti-p53 and anti-Bax antibodies. (E) Mitochondrial cell extracts were prepared from HeLa cells 36 h after transfection, resolved by 12% SDS-PAGE, and subjected to immunoblot analysis using corresponding specific antibodies.
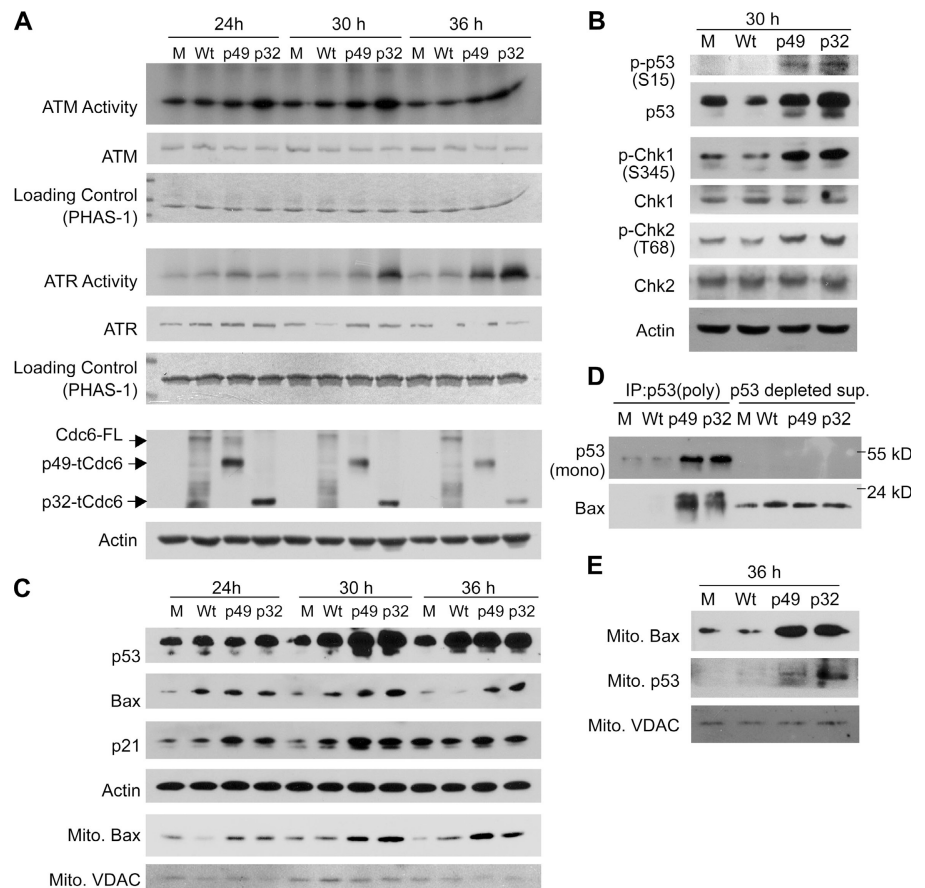
TNF-α–induced apoptosis is strongly enhanced in cells expressing tCdc6, but death is suppressed in cells expressing the uncleavable mutant of Cdc6

We next addressed the possibility that TNF-α–induced cell death is influenced by tCdc6 and Cdc6-UM. TNF-α–induced apoptosis, as measured by caspase-3 activity, was enhanced in cells expressing tCdc6 (Fig. 6 E). In contrast, the tCdc6-induced activation of caspase-3 was suppressed in cells expressing Cdc6-UM to a level that was lower than that exhibited by mock-transfected cells treated with TNF-α but was still much higher than that of unexposed control cells. Thus, we tested whether tCdc6 expression promotes ATM kinase activity during TNF-α–induced apoptosis. Interestingly, this activity was significantly elevated in HeLa cells 2 h after TNF-α treatment (Fig. 6 F). Moreover, TNF-α–induced kinase activation was clearly enhanced by about threefold in cells expressing p32-tCdc6 as compared with that in mock-transfected cells either untreated or treated with TNF-α. Again, TNF-α–induced caspase-3 activity was suppressed in cells expressing Cdc6-UM to levels even lower than those of cells expressing mock or Cdc6-wt (Fig. 6 E). Similarly, TNF-α–induced ATM kinase activity in cells expressing

Cdc6-UM was at the basal level, which was similar to that in cells expressing mock (Fig. 6 G). Nevertheless, the kinase activity in Cdc6-UM–transfected cells was three- to fourfold lower than that in p32-tCdc6–expressed cells after TNF-α treatment. Thus, these results indicate that specific cleavage of Cdc6 is likely functionally linked to ATM kinase activation during TNF-α–induced cell death in HeLa cells.

Down-expression of ATM or ATR suppresses tCdc6- or TNF-α–induced apoptosis

To assess whether ATM or ATR kinase activation might be functionally linked to apoptosis induced by expressing tCdc6 or treatment with TNF-α, the expression level of ATM or ATR kinase was specifically down-regulated using the siRNA technique. 24 h after transfection with siRNA for ATM or ATR, the cells were transfected with pCS2+GFP–Cdc6-wt or –p32-tCdc6. The results indicated that protein levels and the tCdc6-induced activation of ATM or ATR kinase activity were similarly down-regulated to basal levels in the cells by treatment with corresponding siRNA (Fig. 7 A). Moreover, the p32-tCdc6–induced activation of caspase-3 activity was markedly suppressed in the
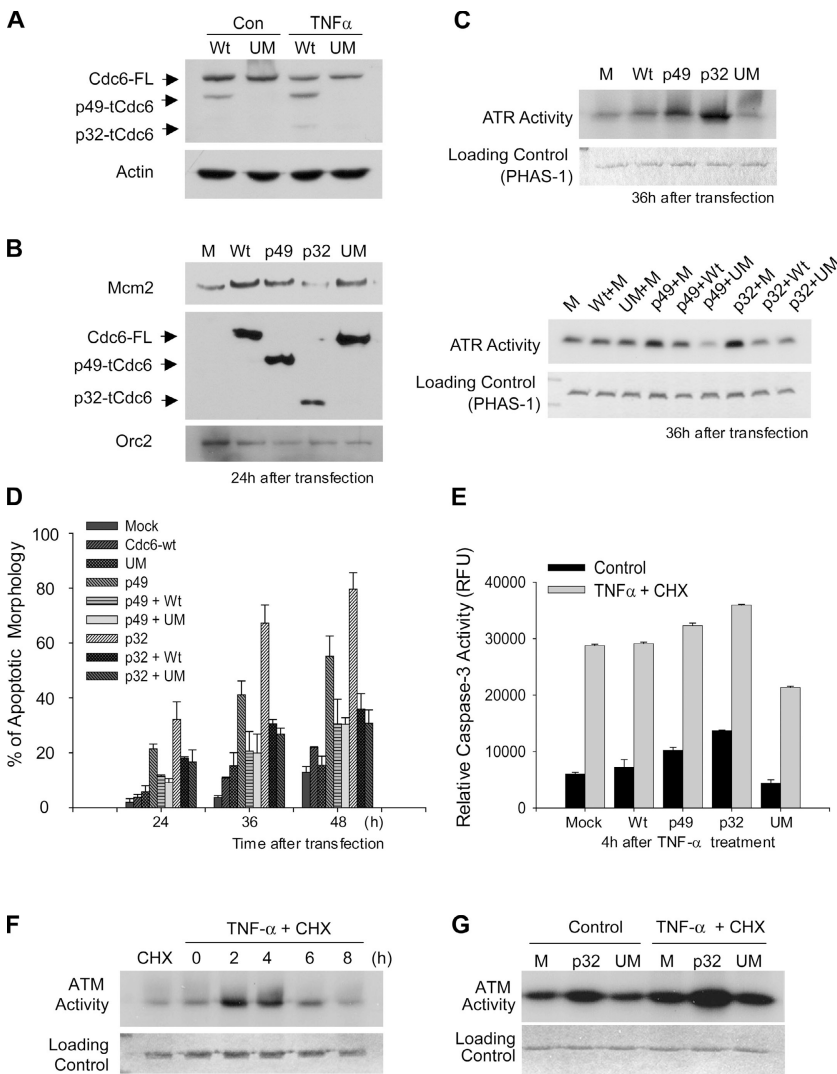

Figure 6. **Proapoptotic effects induced by tCdc6 are blocked in cells expressing caspase-uncleavable Cdc6.** (A) HeLa cells were transfected with cDNA of Cdc6-wt or Cdc6-UM and, after incubating for 24 h, were treated with TNF-α and cycloheximide for 4 h. Cell extracts were subjected to immunoblot analysis using anti-Cdc6 and anti-actin antibodies. (B) Chromatin fractions were prepared 24 h after transfection and subjected to immunoblot analysis using anti-Cdc6, anti-Mcm2, and anti-Orc2 antibodies. (C) HeLa cells were transfected with 3 μg each of pCS2+GFP (M), pCS2+GFP-tagged Cdc6-wt (Wt), tCdc6s (p49 or p32), and Cdc6-UM (UM). When tCdc6s were coexpressed with Cdc6-wt or Cdc6-UM, 3 μg cDNA of each was used. 36 h later, whole cell extracts were prepared and assayed in vitro for ATR kinase activity as described in Fig. 5 A. (D) HeLa cells were transfected with 3 μg each of pCS2+GFP-tagged Cdc6-wt, tCdc6s, and Cdc6-UM. When tCdc6 and Cdc6-wt or Cdc6-UM were cotransfected, 3 μg cDNA of each was used. The percentage of transfected cells exhibiting apoptotic morphology was determined at 24, 36, and 48 h later. The means ± SD (error bars) of data from at least three experiments are shown. (E) 36 h after transfection, HeLa cells were treated with TNF-α and cycloheximide (CHX) for 4 h. Cell extracts were assayed for caspase-3 activity using the fluorogenic caspase-3–specific substrate Ac-DEVD-AFC. RFU, relative fluorescent unit. (F) HeLa cells were treated with TNF-α and cycloheximide for the indicated times, and cell extracts were assayed in vitro for ATM kinase activity as described in Fig. 5 A. (G) 24 h after transfection, HeLa cells were treated with TNF-α and cycloheximide for 2 h, and in vitro ATM kinase activities were similarly assessed by autoradiography.

cells by treatment with siRNA of ATM or ATR (Fig. 7 B). Thus, apoptotic cell death induced by expressing tCdc6 was significantly suppressed by down-expressing ATM or ATR kinase in the cells. Interestingly, in the ATM or ATR down-expressed cells, the levels of caspase-3 activity were even lower than those of cells expressing mock or Cdc6-wt (Fig. 7 B). These results indicated that apoptotic cell death induced by transfection stress alone can be also suppressed by down-expressing ATM or ATR kinase in the cells. We next addressed whether the down-expression of ATM or ATR might also suppress the TNF-α–induced apoptosis. The TNF-α–induced caspase-3 activity was similarly suppressed by ~50% as compared with those in the control siRNA-treated cells by down-expressing ATM or ATR in the cells (Fig. 7 C). These results indicate that activation of ATM and ATR kinase activity is commonly required for tCdc6- or TNF-α–induced apoptosis of the cells.

Collectively, these results indicate that DNA damage–sensing kinase activation may be linked to cellular increases in p53–Bax, which leads to the enhanced mitochondrial translocation of p53 and Bax with subsequent amplification of apoptosis induced by etoposide or TNF-α.

Discussion

We describe a novel functional role for caspase-mediated cleavage of Cdc6 during etoposide- or TNF-α–induced apoptosis. In particular, we show that Cdc6 truncation impairs Mcm2 loading onto chromatin and subsequently activates DNA damage–sensing kinase activities that may be linked to p53–Bax-mediated programmed cell death. Our findings have important implications for the functional role of Cdc6 in apoptosis and also for tCdc6-induced DNA damage signaling in enhancing apoptosis that is induced by treatment with etoposide or TNF-α.

### Caspase-mediated truncation of Cdc6 promotes apoptosis

Previous studies have suggested that Cdc6 is specifically cleaved by caspase-3 during the early stages of apoptosis (Blanchard

et al., 2002; Pelizon et al., 2002; Yim et al., 2003; Schories et al., 2004), which leads to the nuclear accumulation of a tCdc6 fragment, p49-Cdc6, and apoptosis (Yim et al., 2003). Moreover, the expression of a partially uncleavable mutant of HuCdc6 attenuates or delays apoptosis (Pelizon et al., 2002). These results indicate that the caspase-mediated cleavage of Cdc6 protein plays an important role early in apoptosis. Our results demonstrate that the Cdc6 caspase-3 cleavage sites SEVD^{442}/G and DQLD^{290}/S and residues immediately adjacent to these motifs are well conserved among different species (Fig. 1 D). Interestingly, the nuclear level of p32-tCdc6, which is produced by caspase-3 cleavage at the D^{290} residue, is higher by 21% than that of p49-tCdc6, which is produced by cleavage at the D^{442} residue under conditions of elevated cyclin A/Cdk2 activity (Fig. 2). This discrepancy is likely caused by a novel NES sequence located between amino acid residues 290 and 442. Supporting this is that the p49-tCdc6 protein contains a leucine-rich NES-like sequence (consensus NES; LX$_{(1-3)}$LX$_{(2-3)}$LXL, where X is any amino acid; Henderson and Eleftheriou, 2000) in the region of amino acid sequences from 300 to 315 amino acid residues. Moreover, the cytoplasmic translocation of the mutant version of Cdc6 protein, in that leucine residues at 311 and 313 are substituted with alanine residues, decreases by 30% as compared with that of Cdc6-wt in the cells that are overexpressing cyclin A (unpublished data). Apoptosis is more strongly promoted in cells expressing p32-tCdc6 than in cells expressing p49-tCdc6 after treatment with etoposide (Fig. 3). Furthermore, the apoptosis-promoting effects of tCdc6 proteins are consistent with their nuclear localizations (Figs. 2 and 3). These findings thus support our earlier hypothesis that caspase-mediated cleavage of Cdc6 is functionally linked to the promotion of apoptotic progression.

Caspase-mediated cleavage of Cdc6 induces the perturbation of Mcm2 loading onto chromatin

There are several lines of evidence suggesting that the functional perturbation of DNA replication is a key process during

Figure 7. **Down-expression of ATM or ATR suppresses tCdc6- or TNF-α–induced apoptosis.** (A and B) HeLa cells were transfected with a final concentration of 100 nM siRNA duplexes for the control, ATM, or ATR. 24 h thereafter, pCS2+GFP-tagged Cdc6-wt or p32-tCdc6 was transfected. HeLa cell extracts were prepared 30 h after transfection, and whole cell extracts were resolved by 8% SDS-PAGE and subjected to immunoblot analysis with specific antibodies against ATM, ATR, Cdc6, or actin. For ATM or ATR kinase assay in vitro, ATM or ATR kinase was immunoprecipitated with anti-ATM or anti-ATR antibody, and the kinase activity was determined using PHAS-1 as a substrate in the presence of γ-[^{32}P]ATP followed by autoradiography. Proteins were also assayed for caspase-3 activity using the fluorogenic caspase-3–specific substrate Ac-DEVD-AFC. An asterisk denotes endogenous Cdc6. (C) HeLa cells were transfected with a final concentration of 100 nM siRNA duplexes for control, ATM, or ATR. 24 h later, transfected cells were treated with TNF-α and cycloheximide (CHX) for 4 h. Cell extracts were assayed for caspase-3 activity. The means ± SD (error bars) of data from at least three experiments are shown. RFU, relative fluorescent unit.
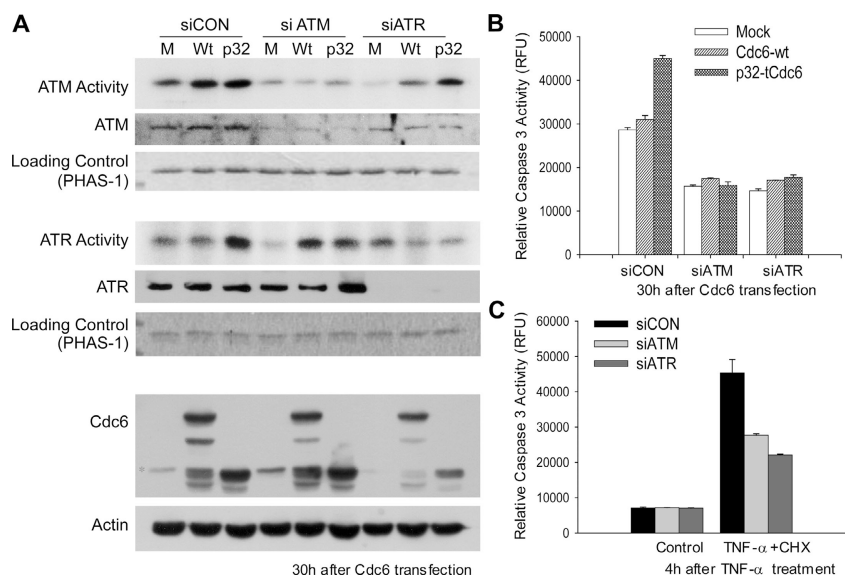
DNA damage–triggered apoptosis. First, apoptosis is induced by defects in the initiation of DNA replication as a result of the *orc2-1* mutation (Weinberger et al., 2005). In addition, temperature-sensitive *orc2-1* mutants cause a defect in a checkpoint and initiation of DNA replication (Weinberger et al., 1999; Trabold et al., 2005). Second, replication initiation proteins are cleaved by caspase during apoptosis (Blanchard et al., 2002; Pelizon et al., 2002; Yim et al., 2003; Schories et al., 2004). Third, when the expression of proteins such as Cdc6, Mcm2, and Cdc45 is blocked by the siRNA technique, proliferation is inhibited, and apoptosis is induced in cancer cells (Feng et al., 2003). Thus, replication fork collapse induced by interfering with the pre-RC may be a general feature of the early stages of apoptosis.

Our results show that the loading of Mcm2 onto chromatin is perturbed during apoptosis induced by etoposide or TNF-α (Fig. 4, A and B). Moreover, this perturbed complex formation is temporally consistent with kinetics of caspase-mediated cleavage of Cdc6 during apoptosis. In addition, the kinetics of chromatin binding indicate that chromatin-bound Mcm2 levels are markedly reduced in cells treated with etoposide or TNF-α. The results also show that the reduced levels of chromatin-bound Mcm2 temporally correlate with elevations in the level of chromatin-bound tCdc6 proteins (Fig. 4, A and B). Thus, the caspase-dependent cleavage of chromatin-bound Cdc6 interferes with the binding of Mcm2 to chromatin and subsequently may perturb pre-RC formation.

Furthermore, ectopically expressed tCdc6 proteins are specifically incorporated into the pre-RC and subsequently inhibit the binding of Mcm2 to chromatin, but they do not interfere with the loading of Orc2 onto chromatin in both asynchronized and early S phase cells (Fig. 4 C). Our results also indicate that the interaction of Mcm2 with tCdc6 proteins is markedly reduced as compared with the Mcm2–Cdc6-wt interaction in transfected cell extracts (Fig. 4 D). These results indicate that the binding of tCdc6 proteins to chromatin interferes with the loading of DNA replication initiation factors, including Mcm2, onto replication complexes, thereby hindering the formation of the DNA pre-RC. Thus, the cleavage of Cdc6 is likely to perturb Mcm2 binding onto chromatin and, consequently, pre-RC formation.

Cleavage of Cdc6 is functionally linked to the activation of ATM/ATR kinase activity

As the Cdc6 cleavage perturbs Mcm2 loading onto chromatin, we assessed whether the cleavage of Cdc6 induces DNA damage. The activities of ATM kinase (Fig. 6 F) and ATR kinase (not depicted) are elevated in HeLa cells during TNF-α–induced apoptosis. Importantly, the activation kinetics of these kinase activities are consistent with those of Cdc6 cleavage in TNF-α–induced apoptosis (Fig. 6). Moreover, as shown in Fig. 5 A, ATR and ATM kinase activities significantly increase in a time-dependent fashion 24–36 h after transfection in tCdc6-expressed cells, whereas their cellular protein levels are minimally altered. Moreover, in cells expressing tCdc6, the phosphorylated levels of Chk1 on S345 residue, Chk2 on T68 residue, and p53 on S15 residue also markedly increase, with kinetics similar to those of the increases in ATR and ATM kinase activities (Fig. 5 B).

Thus, DNA damage–sensing kinases are activated in tCdc6-expressed cells. These results indicate that the expression of tCdc6 is likely to disturb the pre-RC, which then leads to DNA damage with subsequent activation of the DNA damage–sensing kinase activities. However, we do not rule out a possibility that the expression of tCdc6 disrupts chromatin structures but does not induce DNA damage, as ATM activation may result from changes in the structure of chromatin (Bakkenist and Kastan, 2003). We then addressed whether the p53-dependent apoptosis pathway might be involved in Cdc6 cleavage-induced apoptosis. The results suggest that the levels of mitochondrial Bax significantly increase in parallel with increases in the levels of p53 in the tCdc6-expressed cells (Fig. 5 C). Interestingly, the levels of p53 in mitochondria also increase in concert with increases in mitochondrial Bax 36 h after transfection in the tCdc6-expressed cells (Fig. 5 E). Collectively, these results suggest that the expression of tCdc6 induces the perturbation of the loading of Mcm2 onto chromatin, leading to ATM kinase activation, p53 protein stabilization, and, consequently, to apoptosis.

Cdc6-UM suppresses tCdc6-induced ATM/ATR activation and apoptosis

As cells with Cdc6 protein being depleted cannot survive, it is not suitable to use Cdc6 knockout or knock-down for establishing a causal involvement of Cdc6 in the induction of apoptosis. Therefore, we used three different methods to show that the caspase-mediated cleavage of Cdc6 is functionally linked to apoptosis. First, we determined whether the tCdc6-induced apoptotic effects might be prevented in cells that overexpress a caspase-uncleavable Cdc6 mutant (Cdc6-UM). Second, we tested whether the tCdc6-induced apoptotic effects might be functionally linked to the activation of DNA damage–sensing kinase activities and, thereby, to p53–Bax-mediated apoptosis. Third, we assessed whether the TNF-α– or tCdc6-induced apoptotic cell death might be prevented by down-expressing ATM or ATR using the siRNA technique.

Our results show that the chromatin levels of Mcm2 decrease in cells expressing tCdc6 (Fig. 4 C). This tCdc6-induced interference with Mcm2 loading onto chromatin is consistent with the apoptosis-promoting effects induced by tCdc6 (Figs. 3 and 4 C). Importantly, tCdc6-induced apoptosis is efficiently reduced to control levels by the coexpression of Cdc6-UM (Fig. 6 D). Moreover, apoptosis, as assessed by the induction of caspase-3 activity, is prominently enhanced in cells expressing tCdc6 after treatment with TNF-α, and this effect is suppressed in cells expressing Cdc6-UM (Fig. 6 E). Similarly, ATR kinase activity is up-regulated in cells expressing tCdc6, whereas tCdc6-induced kinase activation is effectively prevented in cells that coexpress tCdc6 and Cdc6-UM (Fig. 6 C).

It is noteworthy that the TNF-α–induced activation of ATM is not significantly suppressed to the level of mock-transfected cells in the presence of Cdc6-UM, although ATM kinase activity is markedly up-regulated in TNF-α–treated cells, and that activity further increases in cells expressing p32-tCdc6 (Fig. 6 G). However, the TNF-α–induced proapoptotic effect, as measured by caspase-3 activity, is suppressed by expressing Cdc6-UM (Fig. 6 E). The reason may be explained by the fact

Figure 8. **A model for the mechanism of apoptosis induced by caspase-mediated cleavage of Cdc6.** (Pathway 1) In apoptotic cells, soluble Cdc6, which is cleaved by caspase, cannot bind to preformed pre-RCs but can bind to developing pre-RCs and thus interfere with the binding of MCM to chromatin. (Pathway 2) Caspase cleaves chromatin-bound Cdc6, and the resulting tCdc6 in preexisting pre-RCs induces the dissociation of MCM proteins, whereas tCdc6 in developing pre-RCs inhibits the loading of MCM proteins. The impairment of pre-RC formation then disrupts chromatin structure and/or induces DNA damage with subsequent activation of ATM/ATR activities, leading to p53–Bax-mediated apoptosis.
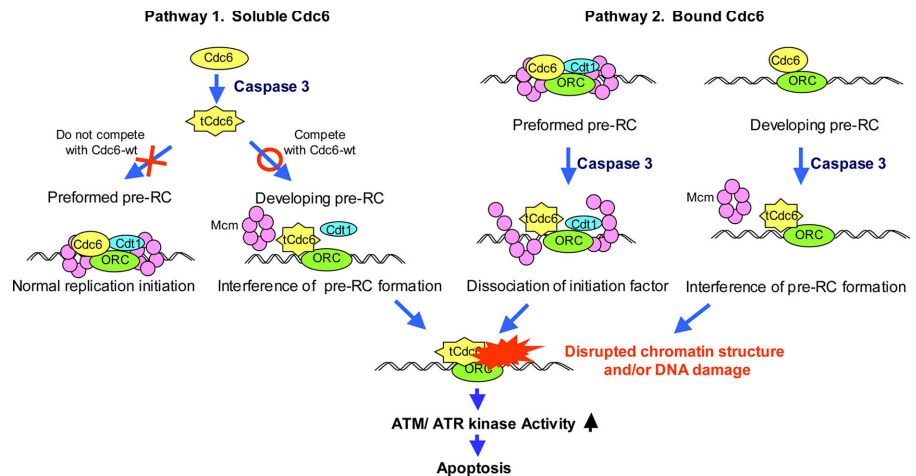
that these assays were measured with the whole cell extracts, which were prepared from the cells that were only partially transfected with Cdc6-UM. Alternatively, the TNF-α–induced caspase-3 activity may also be involved in proteolytic cleavage of chromatin-bound proteins that consequently alters chromatin structures, leading to the activation of ATM kinase.

Collectively, these results suggest that the caspase-mediated cleavage of Cdc6 is not functionally involved in induction but rather facilitates apoptotic progression. Supporting this is that the sequential generation of p49 followed by p32 is not only consistent with kinetics of apoptotic progression in the cells induced by treatment with etoposide or TNF-α but also with their inducing effects on the perturbation of pre-RC formation and on activation of the DNA damage–associated ATM/ATR kinase activity in the cells expressing corresponding tCdc6 proteins. Moreover, the p32-tCdc6– or TNF-α–induced activation of caspase-3 activity is significantly down-regulated as a result of the specific down-expression of ATM or ATR kinase in the cells (Fig. 7). These results indicate that ATM or ATR kinase activity is functionally linked to apoptosis, and the activation of ATM or ATR kinase activity is important to the apoptosis induced by tCdc6 or TNF-α.

Thus, the sequential generation of p49 and p32 protein fragments and their differential effect on the perturbation of Mcm2 loading onto chromatin (and thus of pre-RC and activation of DNA damage–sensing kinase activities) may reflect a possible mechanism that enables the amplification of apoptotic cell death.

A model for the mechanism of tCdc6-induced apoptosis promotion

Our studies suggest that the functional linkages between impairments in pre-RC formation and apoptosis-promoting phenomena are mediated by DNA damage–sensing kinase activities that subsequently regulate the mitochondrial translocation of p53–Bax (Figs. 4 and 5). In this study, we propose a model for the mechanism of the tCdc6-induced apoptotic effects to explain the suppression by Cdc6-UM of apoptosis induced by tCdc6 or by TNF-α treatment (Fig. 8). Pre-RC components are recruited to origins in a stepwise manner, beginning with the

origin RC (ORC). ORC recruits Cdc6 and Cdt1, which are both required for the subsequent loading of MCM proteins (Takeda and Dutta, 2005). Our results show that caspase-generated p49- and p32-tCdc6 are equally capable of binding to the pre-RC (Fig. 4, A and B). Both tCdc6 proteins contain the Walker A domain, a site that is required for ATP and chromatin binding and is essential for the stable interaction among ORC, Cdc6, and MCM proteins, and the Walker B domain, a site that is essential for ATP hydrolysis and MCM protein loading (Fig. 1 E; Herbig et al., 1999; Petersen et al., 1999; Delmolino et al., 2001; Cook et al., 2002; Frolova et al., 2002). However, the truncation of Cdc6 impairs the loading of Mcm2 onto chromatin (Fig. 4, A–C), indicating that the Cdc6 COOH-terminal sequences that are removed by caspase-mediated cleavage may also be required for stable Cdc6–Mcm2 complex formation, as the affinity of tCdc6 proteins for Mcm2 is much lower than that of wt Cdc6 (Fig. 4 D). Thus, the truncation of Cdc6 may remove the Mcm2-binding site on Cdc6 in the pre-RC and consequently hinder the subsequent loading of other initiation factors onto the pre-RC.

The present model illustrates how tCdc6 proteins can induce DNA damage–sensing kinase activities that trigger p53–Bax-mediated apoptosis. As shown in Fig. 8, tCdc6 proteins (pathway 1) cannot compete with Cdc6 in preformed pre-RCs, as Cdc6 is stably bound, whereas they can be inserted into newly forming pre-RCs, which then inhibits subsequent MCM loading (Fig. 8). In pathway 2 (Fig. 8), when Cdc6 in preformed pre-RCs is cleaved by caspase, replication initiation factors such as MCM proteins dissociate from and thereby destabilize the pre-RC. In this case, however, exogenous tCdc6 cannot replace bound tCdc6 in preformed pre-RCs but can replace newly recruited Cdc6 or tCdc6 produced by caspase-mediated cleavage of bound Cdc6. Thus, this model proposes that the expression of tCdc6 impairs newly forming but not previously established pre-RCs. Nevertheless, the caspase-mediated cleavage of Cdc6 in preexisting pre-RCs promotes the dissociation of MCM protein and the subsequent activation of DNA damage–sensing kinase activities. In support of this model, proapoptotic effects induced by tCdc6 expression are completely prevented in cells that coexpress Cdc6-UM, whereas TNF-α–induced effects are only partially suppressed in the presence of Cdc6-UM (Fig. 6).

Also, the activation of ATM/ATR kinase activity is important to promote apoptosis triggered by tCdc6 or TNF-α (Fig. 7).

In summary, our work provides insights into a novel functional role for Cdc6 during apoptosis. Caspase-mediated cleavage of Cdc6, which occurs early in this process, is likely a novel mechanism that promotes or accelerates apoptotic progression during etoposide- or TNF-α–induced apoptosis. Considering these findings together, we propose that Cdc6 may play an important role as a checkpoint to promote apoptosis.

Materials and methods

Materials
DME and FBS were obtained from Invitrogen. The transfection reagent Polyfect was purchased from QIAGEN, and Annexin V AlexaFluor568 was purchased from Roche Diagnostics. Human recombinant TNF-α was obtained from Biosource International. Other chemical reagents were purchased from Sigma-Aldrich.

Plasmids
Human Cdc6 cDNA was provided by R.S. Williams (University of Texas Southwestern Medical Center, Dallas, TX; GenBank/EMBL/DDBJ accession no. NM_001254). Converting the Asp 262, 284, 290, 295, and 442 residues of Cdc6 to Asn was accomplished by altering the Asp codons GAT or GAC to the Asn codons AAT or AAC, respectively, by the megaprimer method (Sambrook and Russell, 2001). The mutation was first introduced by PCR with the mutagenic primers (5′-TGGGAAGAACATGATGAGG-3′, 5′-GGTATTGAACGAGATGG-3′, 5′-TCAACTGAACAGCAAAG-3′, 5′-AGG-CCAGAATGTATTG-3′, 5′-TCAGAAGTTAATGGTAACAGG-3′), the forward primer (5′-AAGGATCCCCTCAAACCCGATCCCAG-3′), and the reverse primer (5′-AAGGATCCT TAAGGCAATCCAG-3′), and the products were cloned into pCITE-4c⁺ for in vitro transcription and translation. Cdc6-AAA (S54A, S74A, and D106A), an unphosphorylatable mutant of Cdc6 by cyclin A/Cdk2 in which Ser 54, 74, and 106 residues of Cdc6 were mutated to Ala, was constructed by sequential single mutation using the PCR method (S54A, 5′-AGCCCTGCCTCTCGCCCCCAGGAAACGT-3′; S74A, 5′-CCCATTTACCTCCTTGTGCTCCACCAAAGCAAGG-3′; and S106A, 5′-AATCAGCTGACAATTAAGGCTCCTAGCAAAAGAGAACTAG-3′). All mutants were confirmed by DNA sequencing. To monitor mammalian expression, Cdc6 was inserted into the vector pCS2+GFP by amplifying full-length Cdc6 cDNA (encoding aa 1–560), p49-tCdc6 cDNA (encoding aa 1–442), or p32-tCdc6 cDNA (encoding aa 1–290). Full-length human cyclin A cDNA was generated by RT-PCR (using oligomers 5′-AAGGATC-CAGCCTATTCTTTGGCC-3′ and 5′-AAGGATCCGGCAGCTGGCATCATT-AATAC-3′ with BamHI sites at the 5′and 3′ ends) and was cloned into the pCMV expression vector.

RNA interference
siRNA duplexes for ATM, ATR, and the control nontargeting siRNA were purchased from Dharmacon. The siRNA sequences (sense strand) for ATM and ATR were UAUAUCACCUGUUUGUUAGUU and GCAACUCGCCUA-ACAGAUAUU, respectively. 5×10^5 HeLa cells in 35-mm dishes were transfected with a final concentration of 100 nM siRNA duplexes using Oligofectamine (Invitrogen) according to the manufacturer's instructions.

Coupled in vitro transcription/translation of Cdc6 and in vitro cleavage assay
The in vitro transcription and translation of cDNAs encoding the human Cdc6 protein and the Cdc6 substitution mutants were performed with the TNT Coupled Reticulocyte Lysate System (Promega) according to the manufacturer's protocols. For in vitro cleavage by caspase-3, 2 μl [^{35}S]methionine-labeled Cdc6 was incubated with 100 ng recombinant caspase-3 as described previously (Yim et al., 2003).

Cell culture, transfection, apoptotic induction, and fluorescence microscopy analysis
Human cervical carcinoma (HeLa) cells were maintained at 37°C and 5% CO_2 as a monolayer culture in DME supplemented with 10% (vol/vol) heat-inactivated FBS, 100 units/ml penicillin, 100 μg/ml streptomycin, and 250 ng/ml amphotericin B. HeLa cells were transfected in 35-mm dishes with 3 μg of the appropriate plasmids using 12 μl Polyfect according

to the manufacturer's instructions. For apoptotic induction, cells were treated with 85 μM etoposide or 5 ng/ml TNF-α and 5 μg/ml cycloheximide. As TNF-α alone had no effect on HeLa cell viability, protein synthesis inhibitor cycloheximide was used together with TNF-α for the induction of apoptosis in HeLa cells (Miura et al., 1995). For DAPI staining, cells were fixed in 4% PFA solution as described previously (Yim et al., 2003).

Annexin V assay
The Annexin V assay was performed as described previously (Yim et al., 2003). The percentage of Annexin V–positive cells and PI-negative cells among GFP-expressing cells was determined by flow cytometry (Particle Analyzing System PAS-III; Partec). Transfected cells were selectively analyzed by gating a subpopulation by forward scatter versus side scatter followed by gating green fluorescence intensity. Because the percentage of Annexin V⁺ cells indicates the frequency of total apoptotic cells and the percentage of PI⁺ cells indicates the frequency of late apoptotic and necrotic cells, the apoptotic index of early apoptotic cell populations was calculated by subtracting the percentage of PI⁺ from the percentage of Annexin V⁺.

FACS analysis
For determination of the sub-G1 fraction as an apoptotic index, cells expressing GFP-tagged proteins were collected over time and fixed in 75% ethanol, stained with 500 μl of 50 μg/ml PI solution, and subjected to FACS analysis. GFP-expressing cells were selectively analyzed for DNA content followed by gating green fluorescence intensity.

Immunoblot analysis and immunoprecipitation pull-down assay
HeLa cells expressing Cdc6 were collected and extracted in lysis buffer (0.5% Triton X-100, 20 mM Tris, pH 7.5, 2 mM MgCl₂, 1 mM DTT, 1 mM EGTA, 50 mM β-glycerophosphate, 25 mM NaF, 1 mM Na vanadate, 2 μg/ml leupeptin, 2 μg/ml pepstatin A, 1 μg/ml antipain, and 100 μg/ml PMSF). Cell lysates were centrifuged at 12,000 rpm for 15 min at 4°C, and the supernatants were collected. After adjusting the protein concentration, proteins were resolved by SDS-PAGE before Western blot analysis with appropriate antibodies. Monoclonal anti-Cdc6, anti-GFP, anti-ATM, anti-p53, and anti-Chk2 antibodies and polyclonal anti-PARP, anti–p-Cdc6 (S54), anti–cyclin A, anti-Cdk2, anti-Chk1, anti-ATM, anti-ATR, anti-Bax, and anti-VDAC antibodies were obtained from Santa Cruz Biotechnology, Inc. Polyclonal phospho-p53 (S15), phospho-Chk2 (T68), and phospho-Chk1 (S345) antibodies were purchased from Cell Signaling Technology. Polyclonal anti-Mcm2 antibody was obtained from BD Biosciences. Immune complexes were revealed using ECL Western blotting detection reagents (Intron Biotechnologies). For immunoprecipitation reaction, p53 or GFP was precipitated from cell lysates with an anti-p53 polyclonal antibody or anti-GFP monoclonal antibody overnight at 4°C with end-over-end mixing followed by incubation with protein A agarose for 2 h at 4°C. Immunoprecipitates were separated from supernatants by centrifugation and washed with lysis buffer. Proteins were extracted from agarose beads by resuspension in 1× laemmli gel-loading buffer and resolved by SDS-PAGE. For the detection of mitochondrial proteins, mitochondrial fractions were extracted in lysis buffer. Mitochondrial proteins were resolved by SDS-PAGE before Western blot analysis with anti-p53, anti-Bax, and anti-VDAC antibodies.

Preparation of nuclear and mitochondrial extracts
Nuclear and mitochondrial extracts were prepared as described previously (Buckley et al., 1999).

Chromatin-binding assay
Chromatin was fractionated with Triton X-100 as described previously (Okuno et al., 2001) with slight modifications. To synchronize 24 h after transfection, cells were treated with 2.5 mM hydroxyurea for 24 h. The nuclear fraction of HeLa cells (2×10^6) expressing Cdc6 was prepared and resuspended in 300 μl Cytoskeleton buffer containing 0.5% Triton X-100. For nuclease digestions, chromatin pellets were resuspended in lysis buffer including 25 units of benzonase nuclease and incubated at 37°C for 10 min followed by chilling on ice and centrifugation. 20 μg of the supernatants were boiled with loading buffer and resolved by 10% SDS-PAGE before Western blot analysis with anti-Cdc6, anti-Orc2, and anti-Mcm2 antibodies.

ATM/ATR kinase assay
ATM or ATR kinase was immunoprecipitated from tCdc6-overexpressing HeLa cells with anti-ATM or anti-ATR polyclonal antibody in buffer (0.5% Triton X-100, 20 mM Tris, pH 7.5, 2 mM MgCl₂, 1 mM DTT, 1 mM EGTA,

50 mM β-glycerophosphate, 25 mM NaF, 1 mM Na₃VO₄, 2 μg/ml leu-peptin, 2 μg/ml pepstatin A, 100 μg/ml PMSF, and 1 μg/ml antipain) followed by incubation with protein A agarose at 4°C for 2 h. The reactions for ATM or ATR kinase activity were performed using 1 μg PHAS-1 (Calbiochem) as a substrate in reaction buffer (50 mM Tris, pH 7.5, 10 mM MgCl₂, 1 mM DTT, 1 mM EGTA, 50 mM β-glycerophosphate, 25 mM NaF, 0.1 mM Na₃VO₄, 1 μg/ml leupeptin, 1 μg/ml pepstatin A, 1 μg/ml antipain, and 100 μg/ml PMSF) containing immunoprecipitated ATM protein or ATR protein and 10 μCi γ-[³²P]ATP at 30°C for 30 min. The reacted samples were suspended in SDS loading buffer, resolved by SDS-PAGE, and detected by autoradiography.

Fluorometric caspase-3 activity assay
50 μg of transfected cell lysates were incubated with 200 nM Ac-DEVD-AFC (BD Biosciences) in reaction buffer (20 mM Hepes, pH 7.4, 100 mM NaCl, 10 mM DTT, 0.1% CHAPS, and 10% sucrose) at 37°C for 1 h. The reaction was monitored by fluorescence emission at 535 nm (excitation at 405 nm).

References

Bakkenist, C.J., and M.B. Kastan. 2003. DNA damage activates ATM through intermolecular autophosphorylation and dimmer dissociation. *Nature*. 421:499–506.

Blanchard, F., M.E. Rusiniak, K. Sharma, X. Sun, I. Todorov, M.M. Castellano, C. Gutierrez, H. Baumann, and W.C. Burhans. 2002. Targeted destruction of DNA replication protein Cdc6 by cell death pathways in mammals and yeast. *Mol. Biol. Cell*. 13:1536–1549.

Buckley, C.D., D. Pilling, N.V. Henriquez, G. Parsonage, K. Threlfall, D. Scheel-Toellner, D.L. Simmons, A.N. Akbar, J.M. Lord, and M. Salmon. 1999. RGD peptides induce apoptosis by direct caspase-3 activation. *Nature*. 397:534–539.

Burhans, W.C., M. Weinberger, M.A. Martchetti, L. Ramachandran, G. D'Urso, and J.A. Huberman. 2003. Apoptosis-like yeast cell death in response to DNA damage and replication defects. *Mutat. Res.* 532:227–243.

Chipuk, J.E., T. Kuwana, L. Bouchier-Hayes, N.M. Drion, D.D. Newmeyer, M. Schuler, and D.R. Green. 2004. Direct Activation of Bax by p53 mediates mitochondrial membrane permeabilization and apoptosis. *Science*. 303:1010–1014.

Cook, J.G., C.H. Park, T.W. Burke, G. Leone, J. DeGregori, A. Engel, and J.R. Nevins. 2002. Analysis of Cdc6 function in the assembly of mammalian prereplication complexes. *Proc. Natl. Acad. Sci. USA*. 99:1347–1352.

Delmolino, L.M., P. Saha, and A. Dutta. 2001. Multiple mechanisms regulate subcellular localization of human Cdc6. *J. Biol. Chem.* 276:26947–26954.

Dodson, G.E., Y. Shi, and R.S. Tibbetts. 2004. DNA replication defects, spontaneous DNA damage, and ATM-dependent checkpoint activation in replication protein A-deficient cells. *J. Biol. Chem.* 279:34010–34014.

Feng, D., Z. Tu, W. Wu, and C. Liang. 2003. Inhibiting the expression of DNA replication-initiation proteins induces apoptosis in human cancer cells. *Cancer Res.* 63:7356–7364.

Frolova, N.S., N. Schek, N. Tikhmyanova, and T.R. Coleman. 2002. Xenopus Cdc6 performs separate functions in initiating DNA replication. *Mol. Biol. Cell*. 13:1298–1312.

Gross, A., J. Jockel, M.C. Wei, and S.J. Korsmeyer. 1998. Enforced dimerization of Bax results in its translocation, mitochondrial dysfunction and apoptosis. *EMBO J.* 17:3878–3885.

Haupt, S., M. Berger, Z. Goldberg, and Y. Haupt. 2003. Apoptosis-the p53 network. *J. Cell Sci.* 116:4077–4085.

Henderson, B.R., and A. Eleftheriou. 2000. A comparison of the activity, sequence specificity, and Crm1-dependence of different nuclear export signals. *Exp. Cell Res.* 256:213–224.

Herbig, U., C.A. Marlar, and E. Fanning. 1999. The Cdc6 nucleotide-binding site regulates its activity in DNA replication in human cells. *Mol. Biol. Cell*. 10:2631–2645.

Kai, M., and T.S. Wang. 2003. Checkpoint responses to replication stalling: including tolerance and preventing mutagenesis. *Mutat. Res.* 532:59–73.

Kaina, B. 2003. DNA damage-triggered apoptosis: critical role of DNA repair, double-strand breaks, cell proliferation and signaling. *Biochem. Pharmacol.* 66:1547–1554.

Liu, Q., S. Guntuku, X.-S. Cui, S. Matsuoka, D. Cortez, K. Tamai, G. Luo, S. Carattini-Rivera, F. DeMayo, A. Bradley, et al. 2000. Chk1 is an essential kinase that is regulated by ATR and required for the G2/M DNA damage checkpoint. *Genes Dev.* 14:1448–1459.

Matsuoka, S., G. Rotman, A. Ogawa, Y. Shiloh, K. Tamai, and S.J. Elledge. 2000. ATM phosphorylates Chk2 in vivo and in vitro. *Proc. Natl. Acad. Sci. USA*. 97:10389–10394.

Miura, M., R.M. Friendlander, and J. Yuan. 1995. Tumor necrosis factor-induced apoptosis is mediated by CrmA-sensitive cell death pathway. *Proc. Natl. Acad. Sci. USA*. 92:8318–8322.

Okuno, Y., A.J. McNairn, N. Elzen, J. Pines, and D.M. Gilbert. 2001. Stability, chromatin association and functional activity of mammalian prereplication complex proteins during cell cycle. *EMBO J.* 20:4263–4277.

Pelizon, C., F.A. Fagagna, L. Farrace, and R.A. Laskey. 2002. Human replication protein Cdc6 is selectively cleaved by caspase-3 during apoptosis. *EMBO Rep.* 3:780–784.

Pereg, Y., D. Shkedy, P. de Graaf, E. Meulmeester, M. Edelson-Averbukh, M. Salek, S. Biton, A.F. Teunisse, W.D. Lehmann, A.G. Jochemsen, and Y. Shiloh. 2005. Phosphorylation of Hdmx mediates its Hdm2- and ATM-dependent degradation in response to DNA damage. *Proc. Natl. Acad. Sci. USA*. 102:5056–5061.

Petersen, B.O., J. Lukas, C.S. Sorensen, J. Bartek, and K. Helin. 1999. Phosphorylation of mammalian Cdc6 by cyclin A/Cdk2 regulates its subcellular localization. *EMBO J.* 18:396–410.

Sambrook, J., and D.W. Russell. 2001. *Molecular Cloning*, 3rd ed.: A Laboratory Cold Spring Harbor Press, Cold Spring Harbor, New York, USA.

Schories, B., K. Engel, B. Dörken, M. Gossen, and K. Bommert. 2004. Characterization of apoptosis-induced Mcm3 and Cdc6 cleavage reveals a proapoptotic effect for one Mcm3 fragment. *Cell Death Differ.* 11:940–942.

Schuler, M., E. Bossy-Wetzel, J.C. Goldstein, P. Fitzgerald, and D.R. Green. 2000. p53 induces apoptosis by caspase activation through mitochondrial cytochrome c release. *J. Biol. Chem.* 275:7337–7342.

Shiloh, Y. 2003. ATM and related protein kinases: safeguarding genomic integrity. *Nat. Rev. Cancer*. 3:155–168.

Takeda, D.Y., and A. Dutta. 2005. DNA replication and progression through S phase. *Oncogene*. 24:2827–2843.

Tercero, J.A., M.P. Longhese, and J.F. Diffley. 2003. A central role for DNA replication forks in checkpoint activation and response. *Mol. Cell*. 11:1323–1336.

Trabold, P.A., M. Weinberger, L. Feng, and W.C. Burhans. 2005. Activation of budding yeast replication origins and suppression of lethal DNA damage effects on origin function by ectopic expression of the co-chaperone protein Mge1. *J. Biol. Chem.* 280:12413–12421.

Weinberger, M., P.A. Trabold, M. Lu, K. Sharma, J.A. Huberman, and W.C. Burhans. 1999. Induction by adozelesin and hydroxyurea of origin recognition complex-dependent DNA damage and DNA replication checkpoints in *Saccharomyces cerevisiae*. *J. Biol. Chem.* 274:35975–35984.

Weinberger, M., L. Ramachandran, L. Feng, K. Sharma, X. Sun, M. Marchetti, J.A. Huberman, and W.C. Burhans. 2005. Apoptosis in budding yeast caused by defects in initiation of DNA replication. *J. Cell Sci.* 118:3543–3553.

Yim, H., Y.H. Jin, B.D. Park, H.J. Choi, and S.K. Lee. 2003. Caspase-3-mediated cleavage of Cdc6 induces nuclear localization of p49-truncated Cdc6 and apoptosis. *Mol. Biol. Cell*. 14:4250–4259.